Laser and Particle Beams (2008), *26*, 461–471. Printed in the USA.

doi:10.1017/S0263034608000475

Planar shock waves in liquids produced by high-energy KrF laser: A technique for studying hydrodynamic instabilities

V.D. ZVORYKIN,[1] L. BERTHE,[2] M. BOUSTIE,[3] A.O. LEVCHENKO,[1] AND N.N. USTINOVSKII[1]

[1]P.N. Lebedev Physical Institute, Russian Academy of Sciences, Moscow, Russia
[2]Laboratoire pour l'Application des Lasers de Puissance, UPR 1576 CNRS, Arcueil CADEX, France
[3]Laboratoire de Combustion et de Détonique, UPR 9028-CNRS, Université de Poitiers-ENSMA, Futuroscope CEDEX, France

(Received 30 January 2008; Accepted 17 June 2008)

Abstract

The paper is devoted to research and development of a novel experimental technique—liquid-filled laser-driven shock tube (LST) for modeling of Rayleigh-Taylor (RT) and Richtmyer-Meshkov (RM) hydrodynamic instabilities development at the contact surface of two immiscible liquids under shock wave (SW) passage. 100-J, 100-ns KrF laser facility GARPUN has been used to irradiate some opaque liquids. A homogenizing focusing system combined multi-element prism raster and a lens to provide non-uniformity less than a few percents across a square 7×7-mm spot, laser intensities being varied in the range of $q = 0.004–2\ \mathrm{GW/cm^2}$. Surface plasma blow-off produced a planar SW, which propagated into the liquid. SW amplitudes as high as 0.8 GPa weakly damping with increasing thickness were measured in dibutyl-phthalate (DBP), which volumetrically absorbed ultraviolet (UV) laser light. Nonlinear absorption coefficients and laser breakdown thresholds were measured for pure water and UV optical materials intended to confine plasma. Test bench experiments were performed to produce standing acoustic waves as initial perturbations at the interface between two immiscible liquids.

Keywords: Immiscible liquids; Instabilities; Liquids; KrF laser; Shock waves

LIQUID-FILLED LASER-DRIVEN SHOCK TUBE CONCEPT

A laser-driven shock tube (LST) has been proposed by Zvorykin and Lebo (2000) as a novel laboratory technique to generate strong shock waves (SW) in gases and liquids by deposition of KrF laser pulse energy on a thin planar layer adjacent to the entrance of a compact gas-filled or liquid-filled cavity. This technique may be applied for studies of various fundamental hydrodynamic phenomena with time scale of several microseconds and space scale of ten millimeters: the development of hydrodynamic instabilities at contact interfaces between different liquids and gases (Cela *et al.*, 2006; Piriz *et al.*, 2006*a*, 2006*b*), hypersonic gas flow around the bodies, effects of strong shock wave refraction and cumulation. These problems are of great importance in inertial confinement fusion (ICF), cosmology, astrophysics, and aerospace engineering (Batani *et al.*, 2007; Gonzalez *et al.*, 2006; Manheimer & Colombant, 2007).

Address correspondence and reprint request to: Vladimir D. Zvorykin, Russian Academy of Sciences, P.N. Lebedev Physical Institute, Leninsky pr. 53, 119991 Moscow, Russia. E-mail: zvorykin@sci.lebedev.ru

The LST concept was first realized in gases. Planar SW with velocities as high as 30 km/s were initiated toward the laser beam by erosion plasma blow-off in rarefied air when 100-J, 100-ns KrF laser pulses irradiated solid targets (Zvorykin *et al.*, 2003, 2004*a*, 2004*b*, 2005; Lebo *et al.*, 2003, 2004; Bakaev *et al.*, 2005; Krasnyuk & Lebo, 2006). In a forward direction, the SW was pushed by thin polystyren (CH) films accelerated by free-expanding plasma up to velocities ~3.5 km/s independently of the gas density. When plasma expansion was confined by a transparent fused silica substrate the velocities increased by a factor 1.3–1.4. A rapid growth of the film thickness from initial few microns to few millimeters was observed during its acceleration (~100 ns) and deceleration (~1 μs) stages, and it was caused by the hydrodynamic instability and turbulent mixing at plasma-film interface. It is well known that a planar interface between two substances undergoing constant or pulsed acceleration exhibits Rayleigh-Taylor (RT) (Taylor, 1950) or Richtmyer-Meshkov (RM) (Richtmyer, 1960; Meshkov, 1969) instabilities. It was shown that any irradiation non-uniformity enhanced instabilities development. A prism-raster focusing system provided large enough ($7 \times 7\ \mathrm{mm^2}$) square irradiation

spot on a target with uniform intensity distribution to ensure initially planar SW generation. The moderate laser intensities $q = 0.1–1\ \mathrm{GW/cm^2}$ and long pulse duration of 100 ns has distinguished our experiments from those performed at the ICF-scale huge powerful lasers with high intensities $q = 1–100\ \mathrm{TW/cm^2}$ and nanosecond pulses (see, i.e., Kilkenny *et al.*, 1994, 2005; Farley *et al.*, 1999; Nobile *et al.*, 2006; Aglitskiy *et al.*, 2006).

A simple but rather informative method to study RT and RM instabilities was implemented in a gravity-accelerated aquarium containing two stratified liquids and bounced on a coil spring (Castilla & Redondo, 1993; Jacobs & Sheely, 1996). Two-liquid system has an advantage in comparison with two-gas system, as it does not need a thin membrane to separate the substances. Thus, the effect of RT and RM instabilities development at liquids interface would be pure of membrane remnants.

In this paper (see also Zvorykin *et al.*, 2008), by an example of dibutyl-phthalate (DBP), which is an opaque liquid for KrF laser radiation at wavelength 248 nm but transparent for visible probe light, we present results on planar SW generation and dynamics aiming afterward to study SW passage through a contact surface with another immiscible liquid. A technique to introduce and to measure controllable sinusoidal perturbations at the contact interface is described. Laser strength and nonlinear absorption in some optical materials and pure deionized water, which can be used as transparent LST windows to increase generated pressure, were measured for 100-ns KrF laser pulses.

GARPUN KrF LASER FACILITY

The layout of target shooting experiments is shown in Figure 1. KrF laser GARPUN operated in injection-controlled regime with a discharge-pumped EMG 150 TMSC master oscillator and electron-beam-pumped $16 \times 18 \times 100$-cm amplifier equipped with an unstable resonator (with magnification factor $M = 6$) (Basov *et al.*, 1993; Zvorykin *et al.*, 2007). It produced laser pulses of $E_{las} = 100$ J energy, with pulse duration at full width at half-maximum (FWHM) $\tau_{las} = 75$ ns and radiation divergence 0.1 mrad at 248-nm wavelength. By increasing a distance between resonator mirrors, an output beam was made slightly convergent. It had a reduced cross section of 10×10 cm when arrived at two-component homogenizing system consisting of a prism raster[1] and a lens (Zvorykin *et al.*, 2004*a*; Bakaev *et al.*, 2005). By splitting an incident beam into 25 individual 2×2-cm beamlets and overlapping them at a focal plane (raster effective focal length $F_{eff} = 1000$ mm) this raster provided non-uniformity less then a few percents across the square spot, which could be resized by adding a focusing lens with an appropriate focal length. For additional $F = 650$ mm lens 7×7-mm spot was obtained. Peak laser intensities $q = E_{las}/S_{las}\tau_{las}$ ($S_{las} = 0.5\ \mathrm{cm^2}$) were varied in the range of $q = 0.004–2\ \mathrm{GW/cm^2}$ by attenuating the incident laser energy.

[1]Authors are grateful to Dr. V.F. Efimkov and Dr. S.I. Mikhailov who has designed the prism raster.

PLASMA AND SW REGISTRATION

Hydrodynamics of laser plasma and SW were investigated by a streak camera or high-speed photo-chronograph with slit-scanning of images by means of a rotating mirror. The schlieren and shadow techniques with a quasi-steady collimated probe beam produced by a capillary-discharge light source were combined with the high-speed slit-scanning recording of images of laser plasma in self luminescence (Fig. 1) (Danilychev & Zvorykin, 1984; Zvorykin & Lebo, 1999; Zvorykin *et al.*, 2004; Bakaev *et al.*, 2005).

Figure 2 demonstrates a slit-scanning image of laser interaction with condensed matter in atmospheric air. The matter was opaque for UV laser radiation, which was absorbed in a thin surface layer and, *vice versa*, was transparent for probe light. Laser pulse formed a plasma plume in evaporated material, which expanded into the ambient air. As a result, a strong SW was generated in the air toward incident laser radiation and a compression wave propagated from the front surface into the solid matter with approximately constant velocity close to sound velocity. A planar SW waveform configuration was observed by the moment when SW propagation length into the matter was less than the laser spot size.

PRESSURE GAUGES AND LAYOUT OF PRESSURE MEASUREMENTS

As for moderate laser intensities of interest, SW velocity weakly depends on the pressure jump at SW front, pressure amplitudes and temporal evolution were measured directly with a piezoelectric gauge. Different techniques were developed earlier to evaluate SW pressure or back-free surface velocities of thin solid targets irradiated by laser pulses. In electromagnetic velocity gauges, a back surface of metal foil was put in contact with two pins, and voltage generated in magnetic field according to Laplace's law was measured (Boustie *et al.*, 1996; Peyre *et al.*, 2000). Interferometer system for any reflector (VISAR) measured Doppler shift of a continuous probe laser beam reflected by the back-free surface of loaded target (Barker & Hollenbach, 1972; Berthe *et al.*, 1997; Tollier *et al.*, 1998). However, the most common technique for shock pressure measurements is piezoelectric gauges. Thin polyvinylidene-fluoride (PVDF) film and its copolymer with trifluoroethylene P(VDF/TrFE) after specific treatments (stretching and subsequent application to electric field) demonstrate strong piezoelectric effect, being the most suitable material to construct different types of pressure gauges (Obara *et al.*, 1995; de Rességuier *et al.*, 1996; Bauer, 2003). The polymer piezoelectric gauges in comparison with more usual X-cut crystalline quartz (Graham, 1975; Fabbro *et al.*, 1990; Devaux *et al.*, 1993)

https://doi.org/10.1017/S0263034608000475 Published online by Cambridge University Press

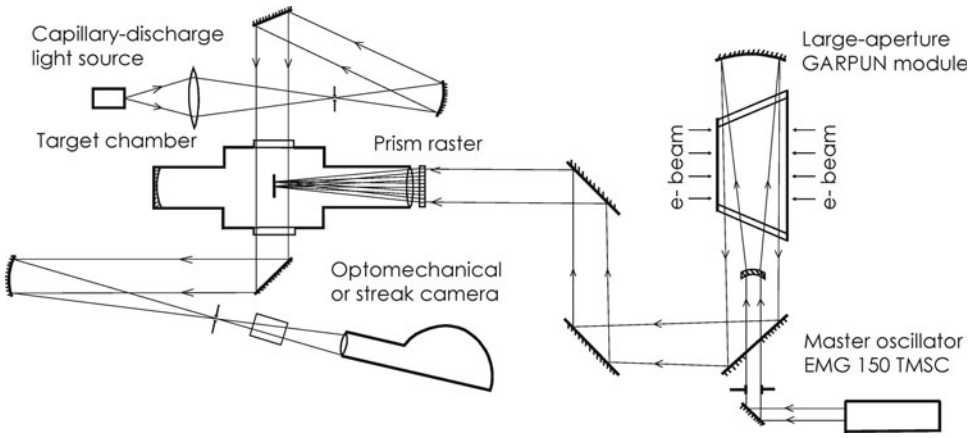

Fig. 1. Layout of target shooting experiments at GARPUN KrF laser facility.

have evident advantages: (1) higher sensitivities, which is important for moderate laser intensities and respectively moderate generated pressures in the presence of a strong parasitic noise; (2) linear response for higher pressure values.

The layout of pressure measurements in dibutyl-phthalate (DBP) is shown in Figure 3. DBP was chosen because it absorbs 248-nm light very strongly. Linear absorption coefficient being measured with a spectrophotometer in a thin cavity of 3.3-μm thickness was about $\alpha = 1.1 \times 10^3\ \mathrm{cm}^{-1}$. No information is available concerning nonlinear absorption in the DBP. However, it is expected to be definitely higher at higher laser intensities. It means the penetration range of laser radiation in our experiments was much less then the spot size and the SW with initially planner front was generated at the liquid surface. Sound velocity in the DBP is $c_1 = 1.408 \times 10^3\ \mathrm{m/s}$ and its density is $\rho_1 = 1.043 \times 10^3\ \mathrm{kg/m}^3$. Those correspond to acoustic impedance of $c_1\rho_1 = 1.47 \times 10^6\ \mathrm{kg} \times \mathrm{s}^{-1} \times \mathrm{m}^{-2}$.

The copolymer pressure gauge assemble was set inside the liquid at various depths from the surface irradiated by the laser. It had 490-μm-thick sensitive element in the form of parallelepiped made of P(VDF/TrFE) with mole composition 77/23%. The outer square 10 × 10-mm electrodes and inner square 4 × 4-mm electrodes were attached to the parallelepiped faces in a guard-ring configuration. The active area of $A = 0.05\ \mathrm{cm}^2$ (shown in Fig. 3 by a dashed line) was defined by the polarized surface in the preliminary poling process. It was slightly less than the inner electrode and thus two-dimensional effects when the SW propagated along-through the sensitive element were eliminated. A specific resin whose acoustic impedance was matched with the copolymer's one filled the transducer body to avoid SW reflection on the rear surface of the copolymer. The calibration test with flyer impacts was carried out earlier that gave for a piezoelectric constant a value $K = 5.35\ \mu\mathrm{C/cm}^2$ (de Rességuier *et al.*, 1996). The transducer current was delivered to Tektronix TDS 2024 scope with 100-Ω twisted-pare cable loaded by two 100-Ω resistors in parallel.

The relationship for the oscilloscope response is given by de Rességuier *et al.* (1996) and Peyre *et al.* (2000)

$$V(t) = -RAK\frac{\Delta u_2(t)}{e_0}, \tag{1}$$

where $V(t)$ is the voltage (V), $R = 50\ \Omega$ is resistance, $e_0 = 0.49 \times 10^{-3}\ \mathrm{m}$ is initial copolymer thickness, and

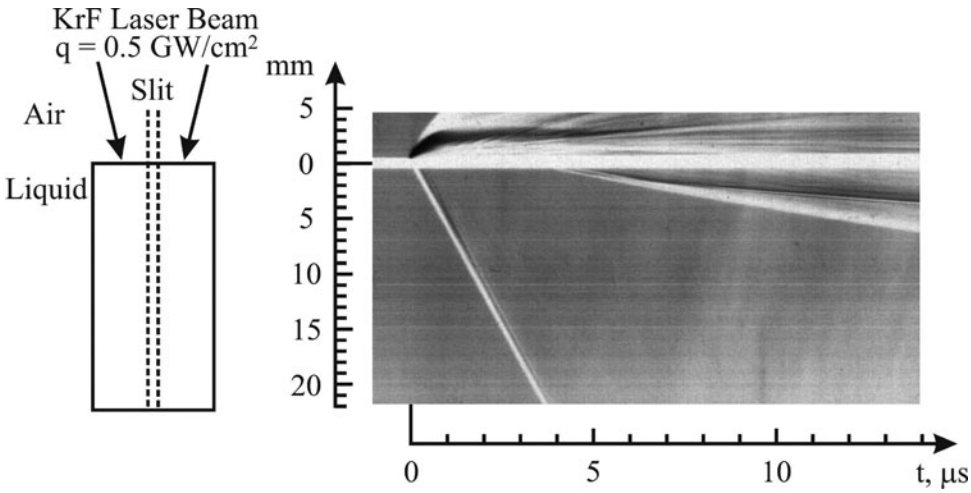

Fig. 2. Combined slit-scanning records of laser plasma (dark in the negative image) and SW (light) propagating from the interface in the ambient air and into condensed matter.

https://doi.org/10.1017/S0263034608000475 Published online by Cambridge University Press

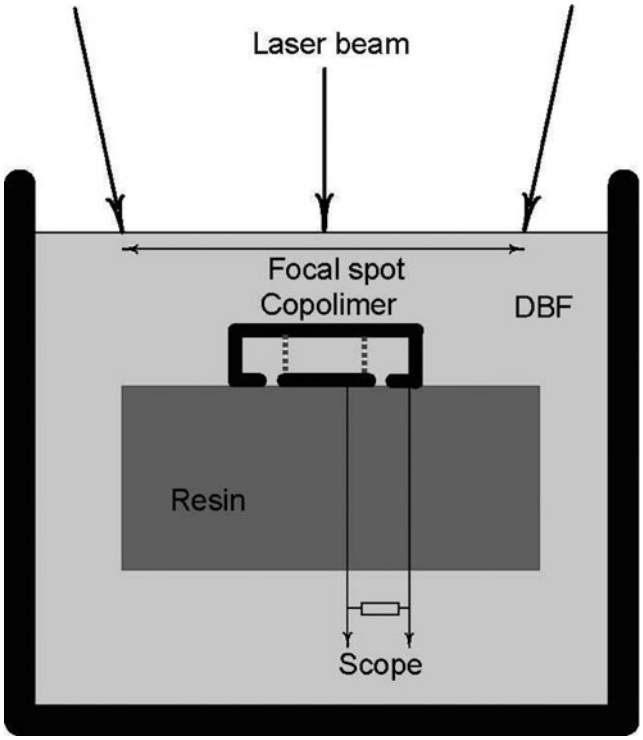

Fig. 3. Layout of pressure measurements in DBP.

$\Delta u_2(t)$ is a difference of material velocities (m/s) at the front and rear surfaces of the sensitive element. Before the SW reaches the rear surface $\Delta u_2 = u_2$, material velocity at the front surface.

Pressure amplitude can be expressed from Hugoniot adiabat of copolymer material

$$P_2 = \rho_2(c_2 + Su_2)u_2, \tag{2}$$

where $\rho_2 = 1.767 \times 10^3$ kg/m^3 is density, $c_2 = 2.579 \times 10^3$ m/s is sound velocity in the copolymer, and $S = 1.586$.

As copolymer acoustic impedance $c_2\rho_2 = 4.56 \times 10^6$ kg $\times$ s^{-1} $\times$ m^{-2} is larger than of DBP, the SW was partially reflected at DBP/copolymer interface giving rise to increased SW amplitude in the copolymer. The relationship between reflected and transmitted SW can be found using $P(u)$ diagram and taking into account that pressures and material velocities at the interface have to comply with a condition of continuity (Zel'dovich & Raizer, 1966). As we did not know Hugoniot adiabat for DBP, we have used its acoustic expression $P_1 = p_1c_1u_1$, which is valid for moderate pressures when $c_1 >> Su_1$ and SW velocity $D_1 = c_1 + Su_1 \approx c_1$ is close to sound velocity.

In the acoustic limit, pressure amplitude in the DBP is less than measured in the copolymer by a factor

$$\frac{P_1}{P_2} = \frac{c_1\rho_1 + c_2\rho_2}{2c_2\rho_2} = 0.66. \tag{3}$$

PRESSURE VS LASER INTENSITY SCALING LAW AND SW GENERATION MECHANISM IN DBP

Typical oscilloscope traces of laser pulse measured by a photodiode and pressure gauge response are shown in Figures 4 and 5 in different time scales. The gauge response behaves as two-polar periodical signal with gradually decreasing amplitude. Time delay τ of the first positive peak relative laser pulse is determined by a passage of the SW through the thickness of DBP. The rise time of pressure $\sim$10 ns is shorter than the leading edge of incident laser pulse. 190-ns width of a positive peak is SW transit time through the copolymer thickness. Negative signal corresponds to a pressure tail when pressure at the front surface of the copolymer becomes less than its preceding values transmitted to the back surface. The second signal with a reversed polarity is delayed by 3τ, and it appears due to a partial reflection of the SW at DBP/copolymer interface

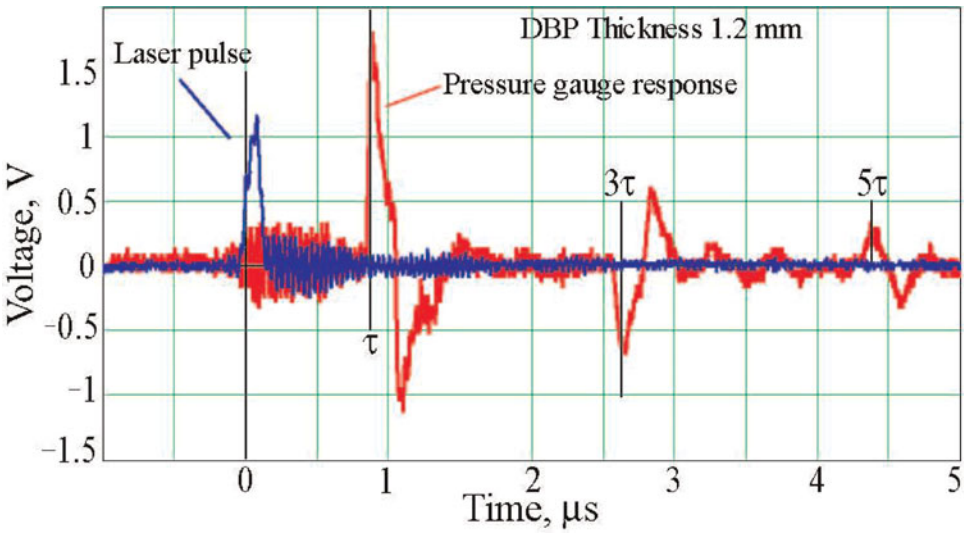

Fig. 4. (Color online) Laser pulse and copolymer gauge response for the DBP thickness of 1.2 mm.

https://doi.org/10.1017/S0263034608000475 Published online by Cambridge University Press

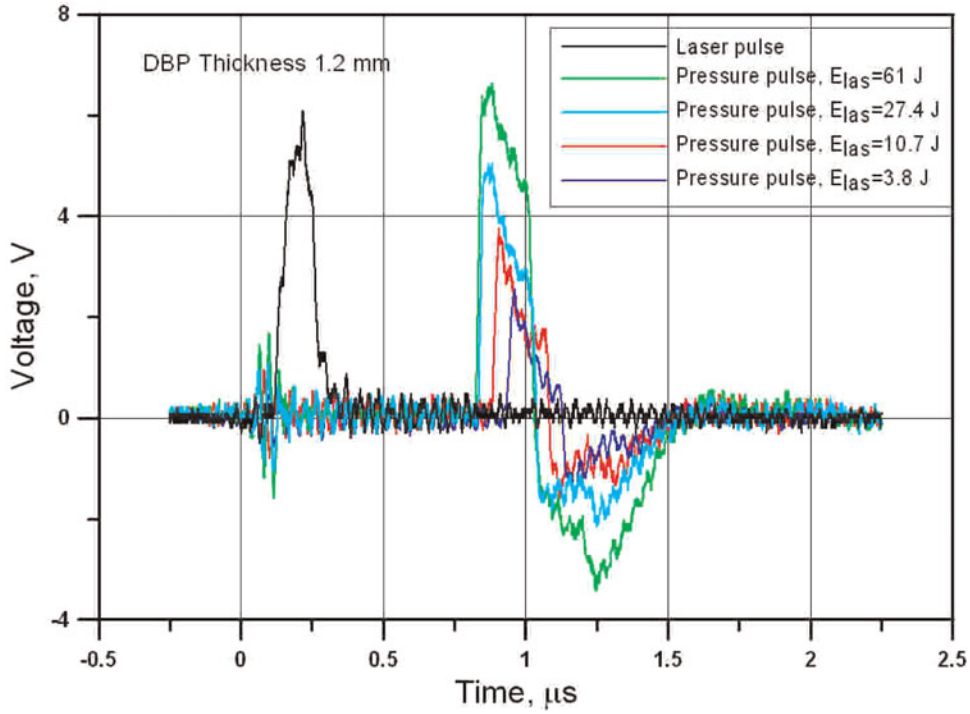

Fig. 5. (Color online) Laser pulse and copolymer gauge response for the DBP thickness of 1.2 mm and different incident radiation energies.

where pressure polarity is conserved and another reflection at the DBP front free-surface where the SW is transformed into a release wave (RW) with an opposite tension. Afterward the same reverberation cycle is repeated with a respective change in signal polarity.

A variation of pressure gauge signals with incident laser energy E_{las} or peak intensity q is demonstrated in Figure 5. Decreasing peak pressure and increasing time delay relative the onset of laser pulse are observed for reduced laser energies. As SW velocity has a minor dependence on SW pressure being approximately equal to sound velocity in DBP, the latter can be only explained by an increasing delay in SW generation for lower laser energies. Some time is required for incident laser flux to heat the surface layer of the DBP up to boiling temperature $t_b = 340^{\circ}$C and to ignite high-pressure plasma in the vapor. This time increases with a reduction of laser energy and the threshold of plasma formation is attained when it becomes comparable with pulse duration. Being reduced to peak laser intensity, it was found to be $q_{th} \approx 0.05$ GW/cm^2.

Peak pressures in the DBP measured at 1.2-mm depth under irradiated surface in dependence on peak laser intensity are shown in Figure 6, and corresponding time delays τ are in Figure 7. The similar dependences have been measured also

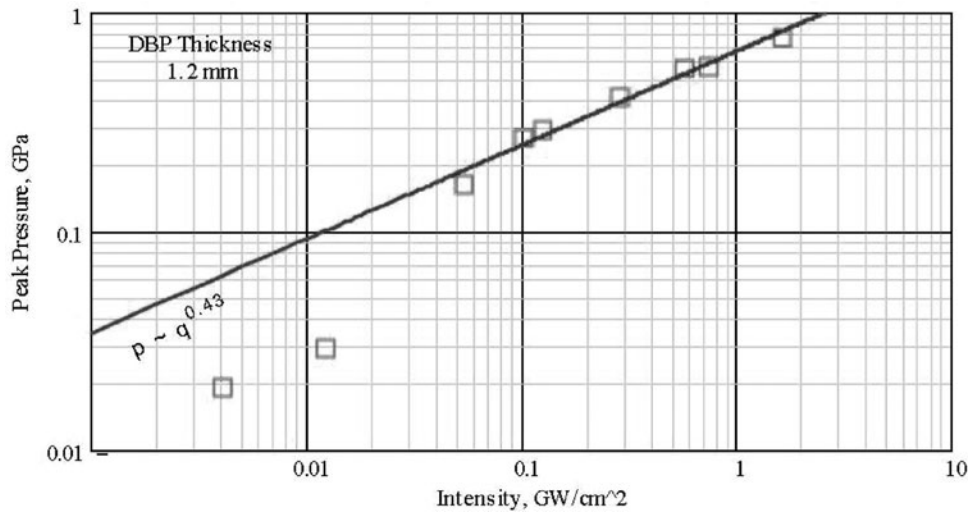

Fig. 6. Peak pressure in DBP measured at 1.2-mm depth versus peak laser intensity.

https://doi.org/10.1017/S0263034608000475 Published online by Cambridge University Press

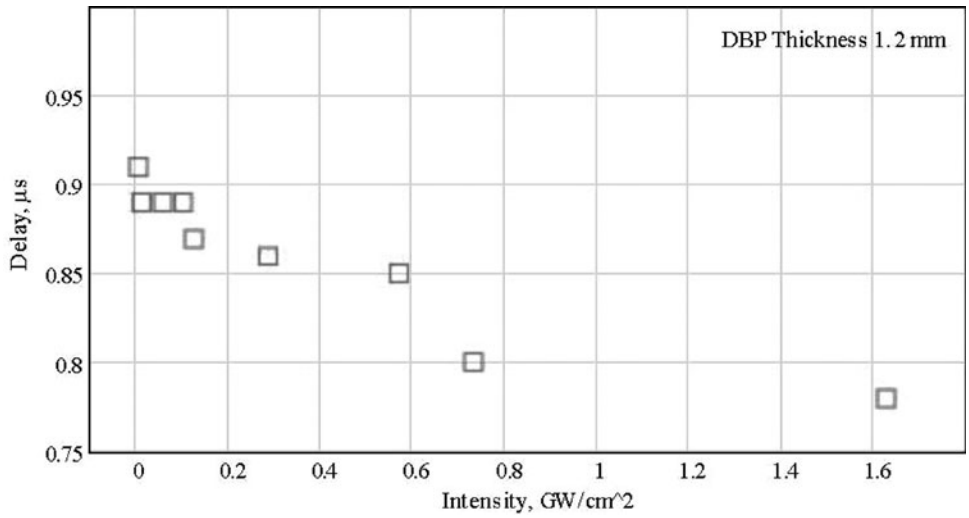

Fig. 7. Time delay of SW arrival relative the onset of laser pulse in DBP at 1.2-mm depth versus peak laser intensity.

for larger depths. Except of low laser intensities $q \leq q_{th}$ the pressure can be approximated by a power law $P \sim q^n$ with an index $n = 0.43 \div 0.46$.

Peak pressure and time delay of the SW in dependence on the DBP thickness beneath irradiated surface are presented in Figures 8 and 9. It is seen that pressure amplitude decreases slowly with the depth while time delay is approximately proportional to DBP thickness.

Many experimental and theoretical studies established a scaling law for the ablation pressure or momentum transferred to planar targets in dependence on laser intensity and laser wavelength (see i.e., Phipps *et al.*, 1988; Zvorykin & Lebo, 1999 and references cited therein). Most of them express this dependence in the form of power law $P \sim q^n \lambda^m$ with indexes varying in the range $n = 0.67 \div 0.80$ and $m = -(0.2 \div 0.3)$. Thus, the present pressure dependence with $n = 0.43 \div 0.46$ contradicts to previous ones. In addition, absolute pressure $p = 0.8$ GPa measured at $q \approx 1\,\mathrm{GW/cm^2}$ is about three times higher then those estimated on the base of previous scaling laws. In our opinion, this difference might originate from the volumetric behavior of absorption of KrF laser radiation in the DBP. Volume absorption arises if the effective deposition depth l_{abs} of incident radiation is significantly larger than the thermal diffusion length during laser-target interaction $x_{th} = 0.969\sqrt{k\tau_{las}}$. Here $k = K/\rho C_v$ represents thermal diffusivity coefficient; ρ, density of target material; C_v, constant-volume specific heat. For typical parameters of organic liquids and laser pulse duration $\tau_{las} = 75$ ns the length of thermal diffusion $x_{th} \approx 10^{-5}$ cm is much less than the penetration range of laser radiation in DBF $l_{abs} = 1/\alpha = 0.9 \cdot 10^{-3}$ cm. According to Phipps *et al.* (1990) the pressure and momentum transfer increase in several times for volume-absorbing substances. In some respect, such regime is close to plasma-confined interaction (see below). A circumstantial evidence for such assumption is the pressure dependence on laser intensity in present experiments, which is close to that for a confined regime described by

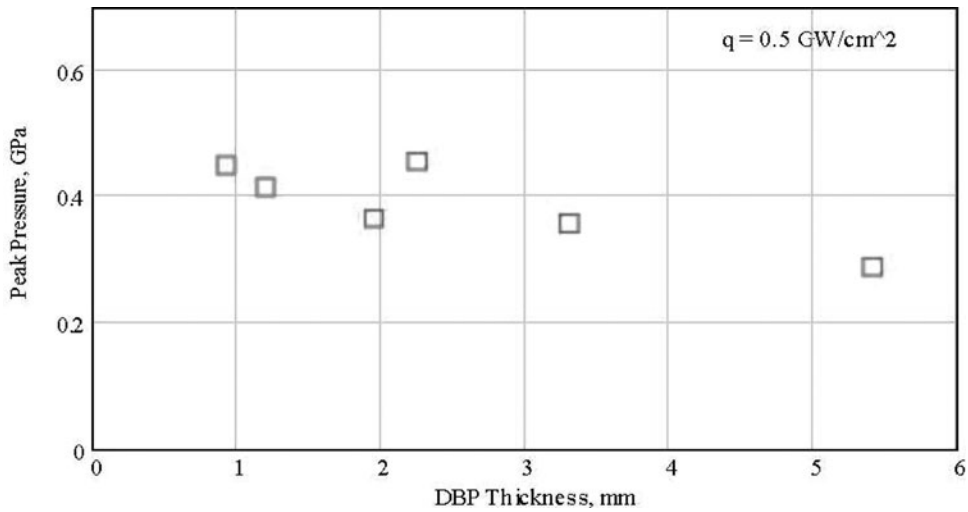

Fig. 8. Peak pressure versus DBP thickness measured at peak laser intensity 0.5 $\mathrm{GW/cm^2}$.

https://doi.org/10.1017/S0263034608000475 Published online by Cambridge University Press

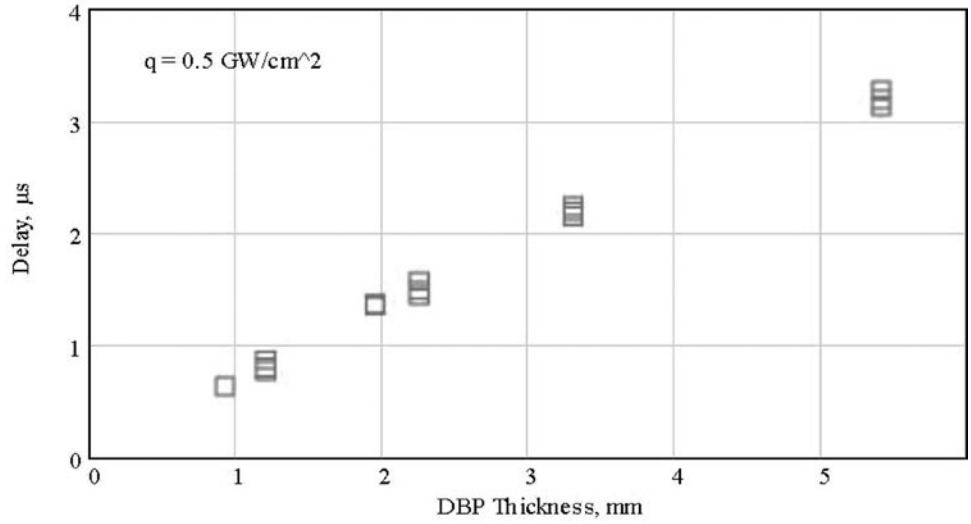

Fig. 9. Time delay of SW arrival relative the onset of laser pulse versus DBP thickness at peak laser intensity 0.5 GW/cm^2.

a power law with an exponent $n = 0.5$ (Anderholm, 1970; Fabbro *et al.*, 1990).

OPTICAL PROPERTIES OF LASER-DRIVEN SHOCK TUBE WINDOWS

The pressure amplitude produced by plasma blow-off might be increased by an order of magnitude if plasma expansion is confined by some transparent solid or liquid material adjacent to evaporated surface. First demonstrated by Anderholm (1970), the effect of water for plasma-confined regime has been further studied with a variety of laser wavelengths (1.064, 0.532, 0.355, and 0.308 μm) and pulse durations (150, 50, 25, 3, 0.6 ns) (Fabbro *et al.*, 1990; Devaux *et al.*, 1993; Boustie *et al.*, 1996; Tollier *et al.*, 1998; Berthe *et al.*, 1999, 2000; Peyre *et al.*, 2000). Breakdown at the front surface of water put a restriction on available laser intensities and highest pressures attained. Unlike the detrimental effect of short laser wavelengths on water breakdown, the confined laser interaction was shown to be more efficient in UV than IR laser irradiation (Berthe *et al.*, 1999).

Linear absorption in pure water for KrF laser radiation is negligible and it can be used as a transparent "window" overlaying the highly absorbing liquid in LST. But nonlinear absorption, being determined for the first time at $\lambda = 248$ nm wavelength for long 100-ns laser pulses in this study, appeared to be rather high and should be taken in consideration. Nonlinear absorption was found in transmission measurements of laser radiation through a cavity of 2-cm length filled with purified deionized water and covered with quartz glass windows. A specific resistance of water being a measure of its purity was $\sim 1\,\mathrm{M}\Omega \times$ cm. Laser beam was focused by the prism raster combined with $F = 2400$ mm lens, which produced uniform irradiation in a square spot of 14×14 mm, twice as much as in DBP shooting experiments. As an effective focal length of the focusing system was 690 mm, much bigger than the cavity length, the spot size was kept constant along the cavity. Incident E_0 and transmitted E_1 laser energies and pulse forms were measured by photodiodes and calorimeters and then they were used to calculate transmittance $T = E_1/E_0$ at corresponding peak laser intensity q.

Figure 10 represents inverse transmittance $1/T = E_0/E_1$ of water-filled cavity in dependence on laser intensity q. Fresnel reflection of the windows is omitted from this graph. It is seen that experimental dots are well approximated by linear dependence $1/T = 1 + \beta l q$, which is typical for two-photon absorption. It is the main absorption process, as the two photons energy $2h\nu = 10$ eV is well above water ionization potential or dissociation energy $\approx$6.5 eV (Reuther *et al.*, 1996). But the found nonlinear absorption coefficient $\beta = 3.9$ cm/GW is at least eight times higher than that measured before in the water for UV laser light at $\lambda = 266$ nm and short pulses of picosecond or femtosecond duration (Nikogosyan & Angelov, 1981; Dragomir *et al.*, 2002). The apparent reason

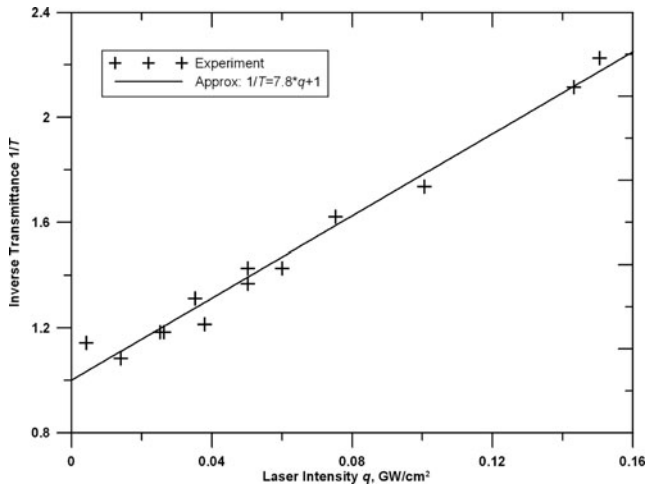

Fig. 10. Inverse transmittance of water-filled cavity in dependence on laser intensity: experimental dots and linear approximation.

https://doi.org/10.1017/S0263034608000475 Published online by Cambridge University Press

Table 1. *Nonlinear absorption coefficient and laser strength of optical materials transparent for KrF laser radiation*

Material	H_2O	SiO_2	MgF_2	CaF_2	BaF_2	Al_2O_3
β, cm/GW	3.9	0.12	0.05	0.03	0.6	2.0
F_{th}, J/cm^2	—	30–40	70	60	—	25
q_{th}, GW/cm^2	—	0.4–0.5	1.0	0.8	—	0.3

is intermediate products formed in primary two-photon ionization and dissociation of water, i.e., H, OH, e^-_{aq}, H_2O_2, H_3O^+, etc., which have long enough lifetime and can additionally absorb KrF laser radiation in a linear process (Reuther *et al.*, 1996).

Nonlinear absorption in water is compared in Table 1 with effective β values for various optical materials suitable for LST window: quartz glass (SiO_2), magnesium fluoride (MgF_2), calcium fluoride (CaF_2), barium fluoride (BaF_2), and synthetic leucosapphire (Al_2O_3) (Eliseev *et al.*, 1996). As $\beta = 0.12$ cm/GW for glass is significantly lower than for water, nonlinear absorption in the cavity windows did not affect on the measured cavity transmittance. Note that the present effective β values for ~100-ns KrF laser pulses are again by an order of magnitude higher than measured earlier at $\lambda = 248$ nm for picosecond and femtosecond laser pulses. Indeed, only SiO_2 band-gap energy of 7.8 eV allows two-photon absorption of KrF quanta while in CaF_2 band-gap energy (10 eV) is just equal to $2h\nu$. Band-gap energies in MgF_2 (11.6 eV) and LiF (11.8 eV) are too wide for direct two-photon absorption. Three-photon absorption was found to be a primary process in these materials, followed by linear absorption at color centers appeared in repetitive irradiations (see i.e., Simon & Gerhardt, 1989; Tomie *et al.*, 1989; Hata *et al.*, 1990). In our case, a quasi-continuous color centers formation during long-pulse KrF samples irradiation apparently increases resulting nonlinear absorption.

Breakdown thresholds F_{th}, [J/cm^2] and q_{th} [GW/cm^2] were also determined for optical materials in large-spot ($S_{las} = 0.5$ cm^2) experiments (Zvorykin *et al.*, 2006), and their values characterize the upper limit of laser intensity attainable in plasma-confined regime with these materials.

STANDING ACOUSTIC WAVES AT LIQUIDS INTERFACE

Figure 11 demonstrates a layout of test bench experiments where sinusoidal standing acoustic waves were produced at the interface between two immiscible liquids by a pair of microphones. They were fed by an audio-frequency oscillator with tunable frequency range 1 Hz–1 kHz. A reflection (or transmission) of expanded probe He-Ne laser beam was used to visualize a pattern of these initial perturbations to be further affected by a compression wave propagating

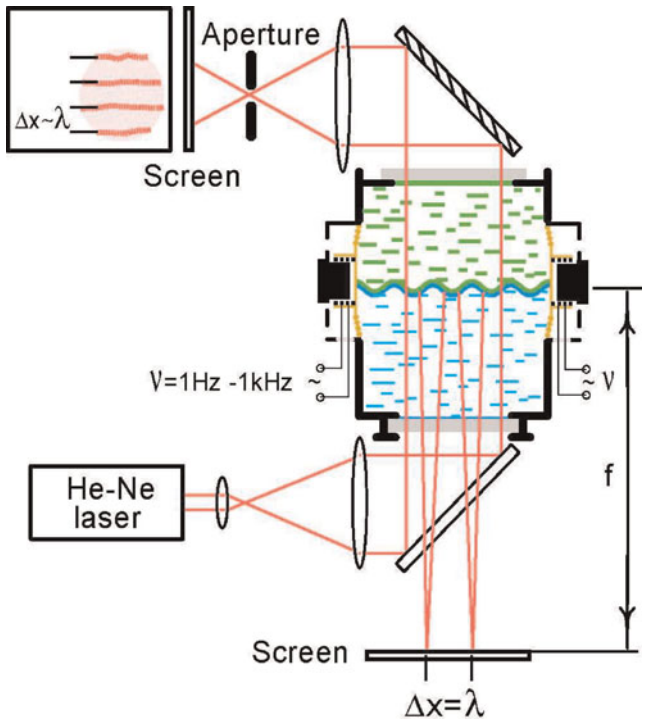

Fig. 11. (Color online) Layout of test-bench experiments with excitation of sinusoidal standing acoustic waves.

from the upper liquid. Standing wave acts like an array of cylindrical mirrors or lenses focusing the light reflected or refracted by liquids interface.

Figure 12 illustrates how a planar probe beam is focused by a sinusoidal surface. The distance where reflected rays intercept with an axis drawn through the sinusoidal maxima is given by the formula

$$f(x, a) = x\frac{1 - (ak)^2 \sin(kx)^2}{2ak \sin kx}, \quad k = \frac{2\pi}{\lambda}. \tag{4}$$

It is seen that most of incident rays would be collected at the distance $f = 1/2ak^2$.

On the screen set in this point distinct strings were observed. By measuring the position of effective focus and interval between the strings, which is equal to excited wavelength, one could find both a wavelength λ (wave number k) and an amplitude a of sinusoidal perturbations. Their values as low as $a*k \sim 10^{-4}$ in product can be easily detected.

Three layers of immiscible liquids with slightly different densities were composed with the upper layer of transparent distillated water (with density $\rho = 1.0$ g/cm^3) for plasma confinement, an opaque mixture of kerosene and chloroform ($\rho = 1.0 \div 1.2$ g/cm^3) for absorbing laser radiation, and a solution of NaCl in the water ($\rho \geq 1.2$ g/cm^3) where hydrodynamic instabilities would be developed.

https://doi.org/10.1017/S0263034608000475 Published online by Cambridge University Press

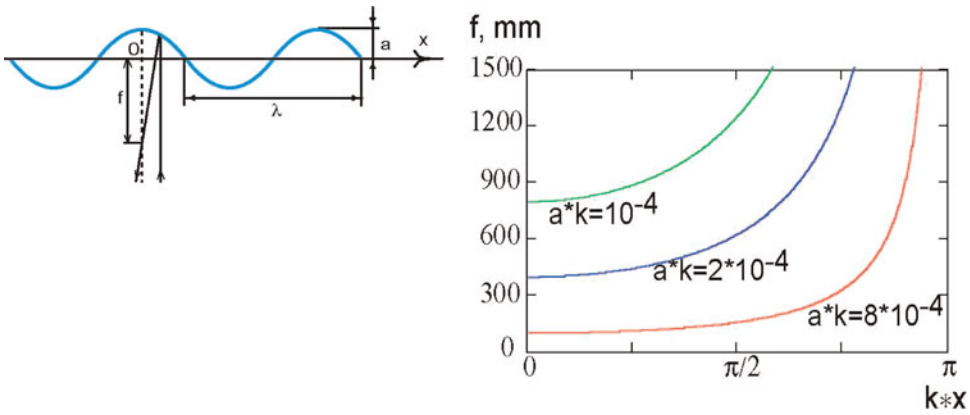

Fig. 12. (Color online) Focusing of planar probe beam by sinusoidal interface.

CONCLUSIONS

Experiments were performed with 100-J, 100-ns KrF laser facility GARPUN to generate planar shock waves in some opaque liquids. Pressure amplitudes up to 0.8 GPa were achieved in dibutyl-phthalate at moderate laser intensities about 1 GW/cm^2 with low damping along the shock wave propagation depth. The scaling law $P \sim q^n$ ($n = 0.43 \div 0.46$) and three-times higher pressure values compared with laser-solid-target interaction are explained by volumetric character of laser radiation absorption. Nonlinear absorption coefficients and laser breakdown thresholds were measured for pure water and optical materials transparent for UV laser radiation. Test bench experiments were performed to produce standing acoustic waves as initial perturbations at the interface between two immiscible liquids. Thus, the necessary experimental data were acquired to suggest a new experimental technique—liquid-filled laser-driven shock tube, which is intended for modeling of RT and RM hydrodynamic instabilities development.

ACKNOWLEDGEMENTS

The authors are grateful to Prof. D. Batani from the University of Milano Bicocca, Italy for his coordination of this research under the INTAS Project 01-0846. Prof. I.G. Lebo from Technical University MIREA promoted our work by useful discussions, and Dr. P.B. Sergeev from P.N. Lebedev Physical Institute provided us with the data on nonlinear absorption in optical materials.

REFERENCES

Aglitskiy, Y., Metzler, N., Karasik, M., Serlin, V., Velikovich, A.L., Obenschain, S.P., Mostovich, A.N., Schmitt, A.J. & Weaver, J. (2006). Perturbation evolution started by Richtmyer-Meshkov instability in planar laser targets. *Phys. Plasmas* **13**, 080703/1–4.

Anderholm, N.C. (1970). Laser-generated stress waves. *Appl. Phys. Lett*. **16**, 113–115.

Bakaev, V.G., Batani, D., Krasnyuk, I.A., Lebo, I.G., Levchenko, A.O., Sychugov, G.V., Tishkin, V.F., Zayarnyi, D.A. & Zvorykin, V.D. (2005). Hydrodynamics of high-energy GARPUN KrF laser interaction with solid and thin-film targets in ambient air. *J. Phys. D: Appl. Phys*. **38**, 2031–2044.

Barker, L.M. & Hollenbach, R.E. (1972). Laser interferometer for measuring high velocities of any reflecting surfaces. *J. Appl. Phys*. **43**, 4669–4675.

Basov, N.G., Bakaev, V.G., Bogdanovskii, A.V., Vadkovskii, A.D., Grigor'yants, E.A., Zvorykin, V.D., Metreveli, G.E., Suchkov, A.F. & Sychugov, G.V. (1993). E-beam pumped "GARPUN" broadband KrF laser with ~1 GW pulsed lasing power. *J. Sov. Laser Res*. **14**, 326–359.

Batani, D., Dezulian, R., Redaelli, R., Benocci, R., Stabile, H., Canova, F., Desai, T., Lucchini, G., Krousky, E., Masek, K., Pfeifer, M., Skala, J., Dudzak, R., Rus, B., Ullschmied, J., Malka, V., Faure, J., Koenig, M., Limpouch, J., Nazarov, W., Pepler, D., Nagai, K., Norimatsu, T. & Nishimura, H. (2007). Recent experiments on the hydrodynamics of laser-produced plasmas conducted at the PALS laboratory. *Laser Part. Beams* **25**, 127–141.

Bauer, F. (2003). PVDF shock compression sensors in shock wave physics. *AIP Conf. Proc*. **706**, 1121–1124.

Berthe, L., Fabbro, R., Peyre, P., Tollier, L. & Bartnicki, E. (1997). Shock waves from water-confined laser-generated plasma. *J. Appl. Phys*. **82**, 2826–2832.

Berthe, L., Fabbro, R., Peyre, P. & Bartnicki, E. (1999). Wavelength dependent of laser shock-wave generation in the water-confinement regime. *J. Appl. Phys*. **85**, 7552–7555.

Berthe, L., Sollier, A., Peyre, P., Fabbro, R. & Bartnicki, E. (2000). The generation of laser shock waves in a water-confinement regime with 50 ns and 150 ns XeCl excimer laser pulses. *J. Phys. D: Appl. Phys*. **33**, 2142–2145.

Boustie, M., Couturier, S., Romain, J.P., Zagouri, D. & Simonnet, H. (1996). Shock pressure and free surface velocity measurements in confined interaction: Response of new VF_2/VF_3 piezoelectric gauges. *Laser Part. Beams* **14**, 171–179.

Castilla, R. & Redondo, J.M. (1993). Mixing front growth in RT and RM instabilities. In *Proc. of the 4th Int. Workshop on the Physics of Compressible Turbulent Mixing*. (Linden, P.F., Youngs, D.L. and Dalziel, S.B. (Eds.), pp. 11–22. Cambridge, UK: Cambridge University Press.

Lopez Cela, J.J., Piriz, A.R., Serna Moreno, M.C. & Tahir, N.A. (2006). Numerical simulations of Rayleigh-Taylor instability in elastic solids. *Laser Part. Beams* **24**, 427–435.

Danilychev, V.A. & Zvorykin, V.D. (1984). Experimental investigation of radiation-gas dynamic processes that develop under the action of high-power $\lambda = 10.6$ μm laser pulses on a solid in a gas. *J. Sov. Laser Res*. **5**, 667–715.

https://doi.org/10.1017/S0263034608000475 Published online by Cambridge University Press

Devaux, D., Fabbro, R., Tollier, L. & Bartnicki, E. (1993). Generation of shock waves by laser-induced plasma in confined geometry. *J. Appl. Phys*. **74**, 2268–2273.

Dragomir, A., McInerney, J.G., Nikogosyan, D.N. & Ruth, A. (2002). Two-photon absorption coefficients of several liquid at 264 nm. *IEEE J. Quant. Electron*. **38**, 31–36.

Eliseev, E.N., Fadeeva, E.I., Zvorykin, V.D., Morozov, N.V., Sagitov, S.I. & Sergeev, P.B. (1996). Laser damage strength of optical materials and coatings for ArF and KrF excimer lasers. *J. Optical Technology* **63**, 136–143.

Fabbro, R., Fournier, J., Ballard, P., Devaux, D. & Virmont, J. (1990). Physical study of laser-produced plasma in confined geometry. *J. Appl. Phys*. **68**, 775–784.

Farley, D.R., Peyser, T.A., Logory, L.M., Muray, S.D. & Burke, E.W. (1999). High Mach number mix instability experiments of an unstable density interface using a single-mode, nonlinear initial perturbation. *Phys. Plasmas* **6**, 4304–4317.

Gonzalez, M., Stehle, C., Audit, E., Busquet, M., Rus, B., Thais, F., Acef, O., Barroso, P., Bar-Shalom, A., Bauduin, D., Kozlova, M., Lery, T., Madouri, A., Mocek, T. & Polan, J. (2006). Astrophysical radiative shocks: From modeling to laboratory experiments. *Laser Part. Beams* **24**, 535–540.

Graham, R.A. (1975). Piezoelectric current from shunted and shorted guard-ring quartz gauges. *J. Appl. Phys*. **46**, 1901–1909.

Hata, K., Watanabe, M. & Watanabe, S. (1990). Nonlinear processes in UV optical materials at 248 nm. *Appl. Phys*. **B 50**, 55–59.

Jacobs, J.W. & Sheely, J.M. (1996). Experimental study of incompressible Richtmyer-Meshkov instability. *Phys. Fluids* **8**, 405–415.

Kilkenny, J.D., Glendinning, S.G., Haan, S.W., Hammel, B.A., Lindl, J.D., Munro, D., Remington, B.A., Weber, S.V., Knauer, J.P. & Verdon, S.V. (1994). A review of the ablative stabilization of the Rayleigh-Taylor instability in regimes relevant to inertial confinement fusion. *Phys. Plasmas* **1**, 1379–1389.

Kilkenny, J.D., Alexander, N.B., Nikroo, A., Steinman, D.A., Nobile, A., Bernat, T., Cook, R., Letts, S., Takagi, M. & Harding, D. (2005). Laser targets compensate for limitations in inertial confinement fusion drivers. *Laser Part. Beams* **23**, 475–482.

Krasnyuk, I.A. & Lebo, I.G. (2006). Comments on the article Hydrodynamics of high-energy GARPUN KrF laser interaction with solid and thin-film targets in ambient air. *J. Phys. D: Appl. Phys*. **39**, 1462–1464.

Lebo, I.G., Iskakov, A.B., Mikhailov, Yu. A., Rozanov, V.B., Starodub, A.N., Sklizkov, G.V., Tishkin, V.F. & Zvorykin, V.D. (2003). Numerical modeling of laser target experiments at "GARPUN" and "PICO" installation. *SPIE* **5228**, 157–163.

Lebo, I.G., Ilyasov, A.O., Iskakov, A.B., Jitkova, O.A., Mikhailov, Yu.A., Rozanov, V.B., Starodub, A.N., Sklizkov, G.V., Tishkin, V.F. & Zorykin, V.D. (2004). Numerical study of laser target experiments at Lebedev Physical Institute. In *Proc. of Third International Conference on Inertial Fusion Sciences and Applications*, pp. 1081–1085, September 7–12, 2003, Monterey, California, USA. American Nuclear Society, Inc.

Manheimer, W. & Colombant, D. (2007). Effects of viscosity in modeling laser fusion implosions. *Laser Part. Beams* **25**, 541–547.

Meshkov, E.E. (1969). Instability of the interface of two gases accelerated by a shock wave. *Izv. Akad. Sci. USSR Fluid Dynamics* **4**, 101–104.

Nikogosyan, D.N. & Angelov, D.A. (1981). Formation of free radicals in water under high-power UV irradiation. *Chem. Phys. Lett*. **77**, 208–210.

Nobile, A., Nikroo, A., Cook, R.C., Cooley, J.C., Alexander, D.J., Hackenberg, R.E., Necker, C.T., Dickerson, R.M., Kilkenny, J.L., Bernat, T.P., Chen, K.C., Xu, H., Stephens, R.B., Huang, H., Haan, S.W., Forsman, A.C., Atherton, L.J., Letts, S.A., Bono, M.J. & Wilson, D.C. (2006). Status of the development of ignition capsules in the US effort to achieve thermonuclear ignition on the national ignition facility. *Laser Part. Beams* **24**, 567–578.

Obara, T., Bourne, N.K. & Mebar, Y. (1995). The construction and calibration of an inexpensive PVDF stress gauge fr fast pressure measurements. *Meas. Sci. Technol*. **6**, 345–348.

Peyre, P., Berthe, L., Fabbro, R. & Sollier, A. (2000). Experimental determination by PVDF and EMV techniques of shock amplitudes induced by 0.6–3 ns laser pulses in a confined regime with water. *J. Phys. D: Appl. Phys*. **33**, 498–503.

Phipps, C.P., Jr., Turner, T.P., Harrison, R.F., York, G.W., Osborne, W.Z., Anderson, G.K., Corlis, X.F., Haynes, L.C., Steele, H.S., Spicochi, K.C. & King, T.R. (1988). Impulse coupling to targets in vacuum by KrF, HF, and CO_2 single-pulse lasers. *J. Appl. Phys*. **64**, 1083–1096.

Phipps, C.P., Jr., Harrison, R.F., Shimada, T., York, G.W., Turner, T.P., Corlis, X.F., Steele, H.S., Haynes, L.C. & King, T.R. (1990). Enhanced vacuum laser-impulse coupling by volume absorption at infrared wavelength. *Laser Part. Beams* **8**, 281–298.

Piriz, A.R., Lopez Cela, J.J., Serna Moreno, M.C., Tahir, N.A. & Hoffmann, D.H.H. (2006*a*). Thin plate effects in the Rayleigh-Taylor instability of elastic solids *Laser. Part. Beams* **24**, 275–282.

Piriz, A.R., Lopez Cela, J.J., Tahir, N.A. & Hoffmann, D.H.H. (2006*b*). Richtmyer-Meshkov flow in elastic solids. *Phys. Rev. E* **74**, 37301/1–4.

de Rességuier, T., Couturier, S., Boustie, M., David, J. & Niérat, G. (1996). Characterization of laser-driven shocks of high intensity using piezoelectric polymers. *J. Appl. Phys*. **80**, 3656–3661.

Reuther, A., Laubereau, A. & Nikogosyan, D.N. (1996). Primary photochemical processes in water. *J. Phys. Chem*. **100**, 16794–16800.

Richtmyer, R.D. (1960). Taylor instability in shock acceleration of compressible fluids. *Commun. Pure Appl. Math*. **23**, 297–319.

Simon, P., Gerhardt, H. & Szatmari, S. (1989). Intensity-dependent loss properties of window materials at 248 nm. *Opt. Lett*. **14**, 1207–1209.

Taylor, G.I. (1950). The instabilities of liquid surfaces when accelerated in a direction perpendicular to their planes. *Proc. Roy. Soc. A* **201**, 192–196.

Tollier, L., Fabbro, R. & Bartnicki, E. (1998). Study of the laser-driven spallation process by the velocity interferometer system for any reflector interferometry technique. I. Laser-shock characterization. *J. Appl. Phys*. **83**, 1224–1230.

Tomie, T., Okuda, I. & Yano, M. (1989). Three-photon absorption in CaF_2 at 248.5 nm. *Appl. Phys. Lett*. **55**, 325–327.

Zel'dovich, Ya.B. & Raizer, Yu.P. (1966). *Physics of Shock Waves and High-Temperature Hydrodynamic Phenomena*. New York: Academic Press.

Zvorykin, V.D. & Lebo, I.G. (1999). Laser and target experiments on KrF GARPUN laser installation at FIAN. *Laser Part. Beams* **17**, 69–88.

Zvorykin, V.D. & Lebo, I.G. (2000). Application of a high-power KrF laser for the study of supersonic gas flows and the development of hydrodynamic instabilities in layered media. *Quant. Electron*. **30**, 540–544.

Zvorykin, V.D., Bakaev, V.G., Iskakov, A.B., Lebo, I.G., Sychugov, G.V. & Tishkin, V.F. (2003). GARPUN KrF-laser-target experiments and numerical simulations on the concept of laser-driven shock tube. *SPIE* **5228**, 151–156.

Zvorykin, V.D., Bakaev, V.G., Lebo, I.G., Sychugov, G.V. (2004*a*). Hydrodynamics of plasma and shock waves generated by high-power GARPUN KrF laser. *Laser Part. Beams* **22**, 51–57.

Zvorykin, V.D., Bakaev, V.G., Batani, D., Lebo, I.G., Levchenko, A.O., Sychugov, G.V., Tishkin, V.F. & Zayarnyi, D.A. (2004*b*). High-Energy GARPUN KrF laser interaction with solid and thin-foil targets in ambient air. *SPIE* **5448**, 654–668.

Zvorykin, V.D., Krasnyuk, I.A., Lebo, I.G. & Levchenko, A.O. (2005). Simulation of the turbulent-mixing region development upon laser acceleration of thin foils. *Bull. Lebedev Phys. Inst*. **9**, 34–41.

Zvorykin, V.D., Bakaev, V.G., Gaynutdinov, R.V., Levchenko, A.O., Sagitov, S.I., Sergeev, P.B., Stavrovskii, D.B. & Ustinovskii, N.N. (2006). Development and evaluation of fluorine-resistant coatings for windows of high-energy KrF laser. *SPIE* **6053**, 60530M/1–9.

Zvorykin, V.D., Didenko, N.V., Ionin, A.A., Kholin, I.V., Konyashchenko, A.V., Krokhin, O.N., Levchenko, A.O., Mavritskii, A.O., Mesyats, G.A., Molchanov, A.G., Rogulev, M.A., Seleznev, L.V., Sinitsyn, D.V., Tenyakov, S.Y., Ustinovskii, N.N. & Zayarnyi, D.A. (2007). GARPUN-MTW: A hybrid Ti: Sapphire/KrF laser facility for simultaneous amplification of subpicosecond/nanosecond pulses relevant to fast-ignition ICF concept. *Laser Part. Beams* **25**, 435–451.

Zvorykin, V., Berthe, L., Boustie, M., Levchenko, A. & Ustinovskii, N. (2008). Dynamics of shock waves generated in liquids by high-energy KrF laser. *SPIE* **6985**, 69850R/1-10.

https://doi.org/10.1017/S0263034608000475 Published online by Cambridge University Press